

Fractional quantum conductance in carbon nanotubes

Stefano Sanvito,^{1,2,3,a} Young-Kyun Kwon,³ David Tománek,³ and Colin J. Lambert¹

¹ *School of Physics and Chemistry, Lancaster University, Lancaster, LA1 4YB, UK*

² *DERA, Electronics Sector, Malvern, Worcs. WR14 3PS, UK*

³ *Department of Physics and Astronomy, and Center for Fundamental Materials Research, Michigan State University, East Lansing, Michigan 48824-1116*

(Received)

Abstract

Using a scattering technique based on a parametrized linear combination of atomic orbitals Hamiltonian, we calculate the ballistic quantum conductance of multi-wall carbon nanotubes. We find that inter-wall interactions not only block some of the quantum conductance channels, but also redistribute the current non-uniformly over the individual tubes across the structure. Our results provide a natural explanation for the unexpected integer and non-integer conductance values reported for multi-wall nanotubes in Ref. [1].

61.48.+c, 72.80.Rj, 73.50.-h, 73.61.Wp

Carbon nanotubes [2,3] are narrow seamless graphitic cylinders, which show an unusual combination of nanometer-size diameter and millimeter-size length. This topology, combined with the absence of defects on a macroscopic scale, gives rise to uncommon electronic properties of individual single-wall nanotubes [4,5], which – depending on their diameter and chirality – can be either conducting or insulating [6–8]. Significant changes in conductivity of these nano-wires may be induced by minute geometric distortions [9] or external fields [10]. More intriguing effects, ranging from the opening of a pseudo-gap at E_F [11,12] to orientational melting [13], have been predicted to occur when identical metallic nanotubes are bundled together in the form of a “rope” [14].

Electron transport in nanotubes is believed to be ballistic in nature, implying the absence of inelastic scattering [1]. Recent conductance measurements of multi-wall carbon nanotubes [1] have raised a significant controversy due to the observation of unexpected conductance values in apparent disagreement with theoretical predictions. In these experiments, multi-wall carbon nanotubes, when brought into contact with liquid mercury, exhibit not only even, but also odd multiples of the conductance quantum $G_0 = 2e^2/h \approx (12.9 \text{ k}\Omega)^{-1}$, whereas the conductance of individual tubes has been predicted to be exactly $2G_0$ [15]. An even bigger surprise was the observation of non-integer quantum conductance values, such as $G \approx 0.5G_0$, since conductance is believed to be quantized in units of G_0 [16].

In this Letter, we demonstrate that the unexpected conductance behavior can arise from the inter-wall interaction in multi-wall or in bundled nanotubes. This interaction may not only block some of the quantum conductance channels, but also redistribute the current non-uniformly over the individual tubes. We show that under the experimental conditions described in Ref. [1], this effect may reduce the conductance of the whole system to well below the expected value of $2G_0$.

The electronic band structure of single-wall [6–8] and multi-wall carbon nanotubes [17–19], as well as single-wall nanotube ropes [11,12] is now well documented. More recently, it has been shown that inter-wall coupling leads to the formation of pseudo-gaps near the Fermi level in multi-wall nanotubes [19] and single-wall nanotube ropes [11,12].

These studies have described infinite periodic structures, the conductance of which is quantized in units of $2G_0$. In what follows, we study the effect of inter-wall coupling on the transport in *finite* structures.

To determine the conductance of finite multi-wall nanotubes, we combine a linear combination of atomic orbitals (LCAO) Hamiltonian with a scattering technique developed recently for magnetic multilayers [20,21]. The parametrization of the LCAO matrix elements, based on *ab initio* results for simpler structures [22], has been used successfully to describe electronic structure details and total energy differences in large systems that were untreatable by *ab initio* techniques. This electronic Hamiltonian had been used previously to explain the electronic structure and superconducting properties of the doped C_{60} solid [23], the opening of a pseudo-gap near the Fermi level in bundled and multi-wall nanotubes [12,19].

The scattering technique, which has recently been employed in studies of the giant magnetoresistance [20,21], determines the quantum-mechanical scattering matrix S of a phase-coherent “defective” region that is connected to “ideal” external reservoirs [20]. At zero temperature, the energy-dependent electrical conductance $G(E)$ is given by the Landauer-Büttiker formula [24]

$$G(E) = \frac{2e^2}{h} T(E) , \quad (1)$$

where $T(E)$ is the total transmission coefficient evaluated at the energy E which, in the case of small bias, is the Fermi energy E_F [25].

For a homogeneous system, $T(E)$ assumes integer values corresponding to the total number of open scattering channels at the energy E . For individual (n,n) “armchair” tubes, this integer is further predicted to be even [15], with a conductance $G = 2G_0$ near the Fermi level. As a reference to previous results [15], the density of states and the calculated conductance of an isolated $(10,10)$ nanotube is shown in Fig. 1.

The corresponding results for the $(10,10)@(15,15)$ double-wall nanotube [19] and the $(5,5)@(10,10)@(15,15)$ triple-wall nanotube, where the inter-wall interaction significantly

modifies the electronic states near the Fermi level, are shown in Fig. 2. The density of states of the double- and the triple-wall nanotubes are shown in Figs. 2(a) and (b), respectively. The corresponding results for the total conductance are given in Figs. 2(c) and (d), respectively. The conductance results suggest that some of the conduction channels have been blocked close to E_F . The inter-wall interaction, which is responsible for this behavior, also leads to a redistribution of the total conduction current over the individual tube walls. The partial conductances of the tube walls are defined accordingly as projections of the total conductance and shown in Fig. 3. We notice that the partial conductance is strongly non-uniform within the pseudo-gaps, where the effects of intertube interactions are stronger.

The experimental set-up of Ref. [1], shown schematically in Fig. 4(a), consists of a multi-wall nanotube that is attached to a gold tip of a Scanning Tunneling Microscope (STM) and used as an electrode. The STM allows the tube to be immersed at calibrated depth intervals into liquid mercury, acting as a counter-electrode. This arrangement allows precise conduction measurements to be performed on an isolated tube. The experimental data of Ref. [1] for the conductance G as a function of the immersion depth z of the tube, reproduced in Fig. 5, suggest that in a finite-length multi-wall nanotube, the conductance may achieve values as small as $0.5G_0$ or $1G_0$.

The key problem in explaining these experimental data is that nothing is known about the internal structure of the multi-wall nanotube or the nature of the contact between the tube and the Au and Hg electrodes. We have considered a number of different scenarios and have concluded that the experimental data can only be explained by assuming that (i) current injection from the gold electrode occurs only into the outermost tube wall, and that (ii) the chemical potential equals that of mercury only within the submersed portion of the tube. In other words, the number of tube walls in contact with mercury depends on the immersion depth. The first assumption implies that the electrical contact between the tube and the gold electrode involves only the outermost wall, as illustrated in Fig. 4(a). The validity of the second assumption – in spite of the fact that mercury only wets the outer tubes – is justified by the presence of the inter-wall interaction. The main origin of the

anomalous conductance reduction, to be discussed below, is the backscattering of carriers at the interface of two regions with different numbers of walls due to a discontinuous change of the conduction current distribution.

The conductance calculation is then reduced to a scattering problem involving a semi-infinite single-wall nanotube (the one in direct contact with gold) in contact with a scattering region consisting of an *inhomogeneous* multi-wall tube and the Hg reservoir as the counter-electrode. Depending on the immersion depth, denoted by Hg(#1), Hg(#2), and Hg(#3) in Fig. 4(a), portions of the single-wall, the double-wall, and even the triple-wall sections of the tube are submersed into mercury. Our calculations are performed within the linear-response regime and assume that the entire submersed portion of the tube is in “direct contact”, i.e. equipotential with the mercury. Increasing the immersion depth from Hg(#1) to Hg(#2) and Hg(#3), an increasing number of walls achieve “direct contact” with mercury, thereby changing the total conductance $G(E)$, as shown in Figs. 4(b)-(d) and Fig. 5. We also notice that the conductance of the inhomogeneous multi-wall structure of Fig. 4(a) cannot exceed that of a single-wall nanotube, which is the only tube in electrical contact with the gold electrode.

The calculation underlying Fig. 4(b) for the submersion depth Hg(#1) considers a scattering region consisting of a finite-length $(5,5)@(10,10)@(15,15)$ nanotube connected to another finite segment of a $(10,10)@(15,15)$ nanotube. This scattering region is then connected to external semi-infinite leads consisting of $(15,15)$ nanotubes. The calculation for the submersion depth Hg(#2), shown in Fig. 4(c), considers a scattering region formed of a finite-length $(5,5)@(10,10)@(15,15)$ nanotube segment that is attached to a $(15,15)$ nanotube lead on one end and to a $(10,10)@(15,15)$ nanotube lead on the other end. Results in Fig. 4(d) for the submersion depth Hg(#3) represent the conductance of a $(5,5)@(10,10)@(15,15)$ nanotube lead in contact with a $(15,15)$ nanotube lead. The calculated conductances depend on the position of the Fermi level within the tube. Even though E_F may vary with the immersion depth due to a changing contact potential, we expect these changes to lie within the narrow energy window of ≈ 0.05 eV, indicated by the shaded region. Our results

of Figs. 4(b)-(d), suggesting discrete conductance increases from $G \approx 0.5G_0$ for Hg(#1) to $G \approx 1G_0$ for Hg(#2) and Hg(#3) are in excellent agreement with the recent experimental data of Ref. [1], presented in Fig. 5.

It is essential to point out that from our calculations we expect a conductance value $G \approx 0.5G_0$ only when a single tube wall is in direct contact with mercury. In the case that a single-wall region is long, we expect this small conductance value to extend over a large range of immersion depths [1]. In absence of such a single-wall segment, we expect for the conductance only values of $1G_0$ and above. We believe that the anomalous sample-to-sample variation of the observed conductance [1] is related to the structural properties of the nanotube and not to defects which are believed to play only a minor role in transport [26].

We also want to point out that a very different conductance behavior is expected when more than one tube wall is in direct contact with the Au electrode. As a possible scenario, we consider an inhomogeneous nanotube similar to that in Fig. 4(a), where now all of the three tube walls are in direct contact with the gold electrode. With two conduction channels per tube wall, the conductance has an upper bound of $6G_0$. Calculations analogous to those presented in Fig. 4 suggest a minimum conductance value $G \approx 1G_0$ to occur for a finite-length (10,10)@(15,15) tube segment sandwiched between (15,15) and (5,5)@(10,10)@(15,15) nanotube leads, representing the smallest submersion depth Hg(#1), with mercury in direct contact with only the single-wall portion of the tube. The conductance value $G \approx 2G_0$ is obtained for a (10,10)@(15,15) nanotube lead in contact with a (5,5)@(10,10)@(15,15) nanotube lead, representing submersion depth Hg(#2), with mercury in direct contact with a double-wall tube segment. Finally, depending on the position of E_F , the conductance of a triple-wall nanotube submersed in mercury, modeled by an infinite (5,5)@(10,10)@(15,15) tube, may achieve conductance values of $4G_0$ or $6G_0$. Even though the inter-wall interaction leads to a significant suppression of the conductance, the predicted increase in the conductance from $1G_0$ to $2G_0$ and $4G_0 - 6G_0$ with increasing submersion depth is much larger than in the scenario of Fig. 4. Also the predicted conductance values are very different from the

experimental data of Ref. [1], thus suggesting that only the outermost tube is in electrical contact with the gold electrode.

In conclusion, we have shown that the inter-wall interaction in multi-wall nanotubes not only blocks certain conduction channels, but also re-distributes the current non-uniformly across the walls. We have calculated conductance in several structures and concluded that the puzzling observation of fractional quantum conductance in multi-wall nanotubes can be explained by assuming that only the outermost tube wall is in electrical contact with the gold electrode. Moreover, we have shown that the sample-to-sample variations in the conductance are entirely related to the structure of the nanotube. A very similar behavior is expected for bundled single-wall tubes of different length submersed into Hg or another metal. These predictions raise important questions concerning the nature of the nanotube/metal interface, which deserve further investigation both experimentally and theoretically.

We acknowledge fruitful discussions with Walt de Heer. This work has been done in collaboration with the group of J.H. Jefferson at DERA. SS acknowledges financial support by the DERA and the MSU-CMPT visitor fund. YKK and DT acknowledge financial support by the Office of Naval Research under Grant Number N00014-99-1-0252.

REFERENCES

^a Corresponding author. E-mail: sanvito@dera.gov.uk

- [1] Stefan Frank, Philippe Poncharal, Z.L. Wang, and Walt A. de Heer, *Science* **280**, 1744 (1998).
- [2] S. Iijima, *Nature* **354**, 56 (1991).
- [3] For a general review, see M.S. Dresselhaus, G. Dresselhaus, and P.C. Eklund, *Science of Fullerenes and Carbon Nanotubes* (Academic Press Inc., 1996 San Diego), and references therein.
- [4] S. Iijima and T. Ichihashi, *Nature* **363**, 603 (1993).
- [5] D.S. Bethune, C.H. Kiang, M.S. de Vries, G. Gorman, R. Savoy, J. Vazquez, R. Beyers, *Nature* **363**, 605 (1993).
- [6] J.W. Mintmire, B.I. Dunlap, and C.T. White, *Phys. Rev. Lett.* **68**, 631 (1992).
- [7] R. Saito, M. Fujita, G. Dresselhaus, and M.S. Dresselhaus, *Appl. Phys. Lett.* **60**, 2204 (1992).
- [8] N. Hamada, S. Sawada, and A. Oshiyama, *Phys. Rev. Lett.* **68**, 1579 (1992).
- [9] C.L. Kane and E.J. Mele, *Phys. Rev. Lett.* **78**, 1932 (1997); Alain Rochefort, Dennis Salahub, and Phaedon Avouris, *Chem. Phys. Lett.* **297**, 45 (1998).
- [10] S.J. Tans, A.R.M. Verschueren, and C. Dekker, *Nature* **393**, 49 (1998).
- [11] P. Delaney, H.J. Choi, J. Ihm, S.G. Louie, and M.L. Cohen, *Nature* **391**, 466 (1998).
- [12] Young-Kyun Kwon, Susumu Saito, and David Tománek, *Phys. Rev. B* **58**, R13314 (1998).
- [13] Young-Kyun Kwon, David Tománek, Young Hee Lee, Kee Hag Lee, and Susumu Saito, *J. Mater. Res.* **13**, 2363 (1998).

- [14] A. Thess, R. Lee, P. Nikolaev, H. Dai, P. Petit, J. Robert, C. Xu, Y.H. Lee, S.G. Kim, D.T. Colbert, G. Scuseria, D. Tománek, J.E. Fischer, and R.E. Smalley, *Science* **273**, 483 (1996).
- [15] L. Chico, L.X. Benedict, S.G. Louie and M.L. Cohen, *Phys. Rev. B* **54**, 2600 (1996), W. Tian and S. Datta, *ibid.* **49**, 5097 (1994), M.F. Lin and K.W.-K. Shung, *ibid.* **51**, 7592 (1995).
- [16] R. Landauer, *Phil. Mag.* **21**, 863 (1970).
- [17] Riichiro Saito, G. Dresselhaus, and M.S. Dresselhaus, *J. Appl. Phys.* **73**, 494 (1993).
- [18] Ph. Lambin, L. Philippe, J.C. Charlier, and J.P. Michenaud, *Comput. Mater. Sci.* **2**, 350 (1994).
- [19] Young-Kyun Kwon and David Tománek, *Phys. Rev. B* **58**, R16001 (1998).
- [20] S. Sanvito, C.J. Lambert, J.H. Jefferson, A.M. Bratkovsky, *Phys. Rev. B* **59**, 11936 (1999).
- [21] S. Sanvito, C.J. Lambert, J.H. Jefferson, A.M. Bratkovsky, *J. Phys. C: Condens. Matter.* **10**, L691 (1998).
- [22] D. Tománek and Michael A. Schluter, *Phys. Rev. Lett.* **67**, 2331 (1991).
- [23] M. Schluter, M. Lannoo, M. Needels, G.A. Baraff, and D. Tománek, *Phys. Rev. Lett.* **68**, 526 (1992).
- [24] M. Büttiker, Y. Imry, R. Landauer, S. Pinhas, *Phys. Rev. B* **31**, 6207 (1985).
- [25] When calculating the S -matrix of a doubly-infinite nanotube, comprising a scattering region connected to two semi-infinite single- and multi-wall nanotube leads, we note that the unit cell in each segment consists of two atomic planes along the nanotube axis. Since the hopping matrix between adjacent unit cells (H_1 in Ref. [20]) is singular in this case, we first project out the non-coupled degrees of freedom before calculating

the scattering channels.

- [26] T. Ando, and T. Nakanishi, J. Phys. Soc. Jpn. **67**, 1704 (1998) and T. Ando, T. Nakanishi, R. Saito, *ibid.* **67**, 2857 (1998).

FIGURES

FIG. 1. Electronic density of states (DOS) (a) and conductance G (b) of an isolated single-wall (10,10) carbon nanotube. The DOS is given in arbitrary units, and G is given in units of the conductance quantum $G_0 = 2e^2/h \approx (12.9 \text{ k}\Omega)^{-1}$.

FIG. 2. Electronic density of states and conductance of a double-wall (10,10)@(15,15) nanotube [(a) and (c), respectively], and a triple-wall (5,5)@(10,10)@(15,15) nanotube [(b) and (d), respectively].

FIG. 3. Partial conductance of the constituent tubes of (a) a double-wall (10,10)@(15,15) nanotube and (b) a triple-wall (5,5)@(10,10)@(15,15) nanotube. Values for the outermost (15,15) tube are given by the solid line, for the (10,10) tube by the dashed line, and for the innermost (5,5) tube by the dotted line.

FIG. 4. (a) Schematic geometry of a multi-wall nanotube that is being immersed into mercury up to different depths labeled Hg(#1), Hg(#2), and Hg(#3). Only the outermost tube is considered to be in contact with the gold STM tip on which it is suspended. The conductance of this system is given in (b) for the immersion depth Hg(#1), in (c) for Hg(#2), and in (d) for Hg(#3) as a function of the position of E_F . The Fermi level may shift with changing immersion depth within a narrow range indicated by the shaded region.

FIG. 5. Conductance G of a multi-wall nanotube as a function of immersion depth z in mercury. Results predicted for the multi-wall nanotube discussed in Fig. 4, given by the dashed line, are superimposed on the experimental data of Ref. [1].

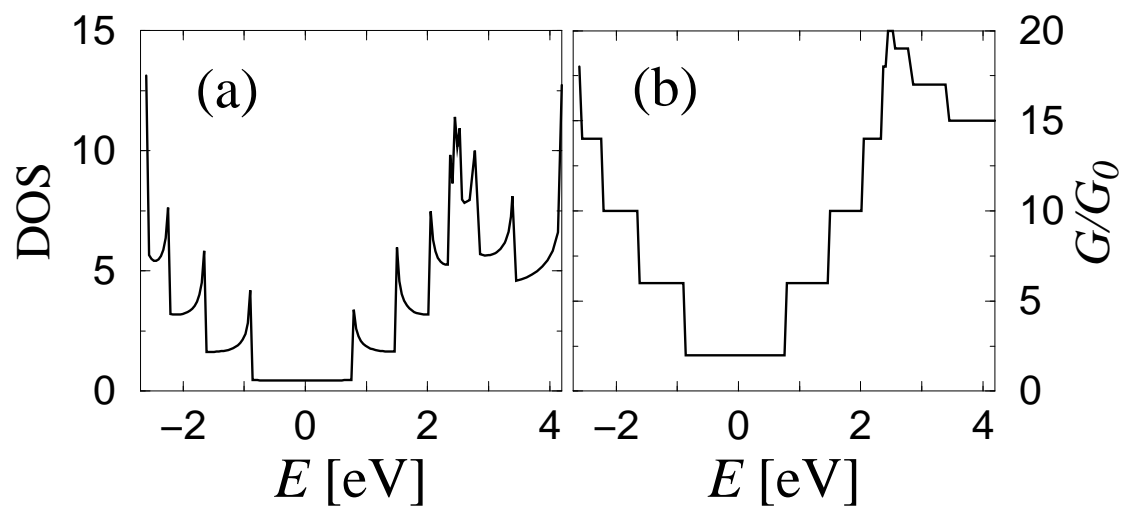


Figure 1

(Stefano Sanvito, Young-Kyun Kwon, David Tománek, and Colin J. Lambert,
“Fractional quantum conductance in carbon nanotubes”)

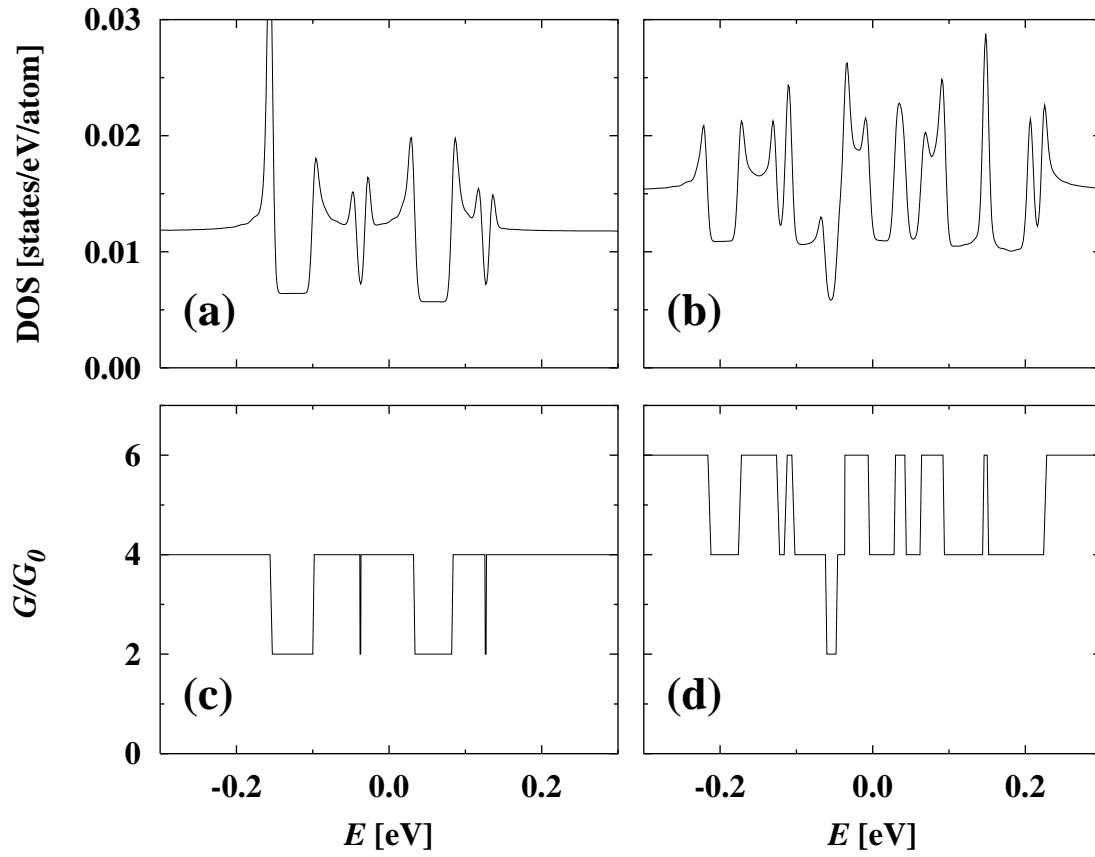


Figure 2

(Stefano Sanvito, Young-Kyun Kwon, David Tománek, and Colin J. Lambert,
“Fractional quantum conductance in carbon nanotubes”)

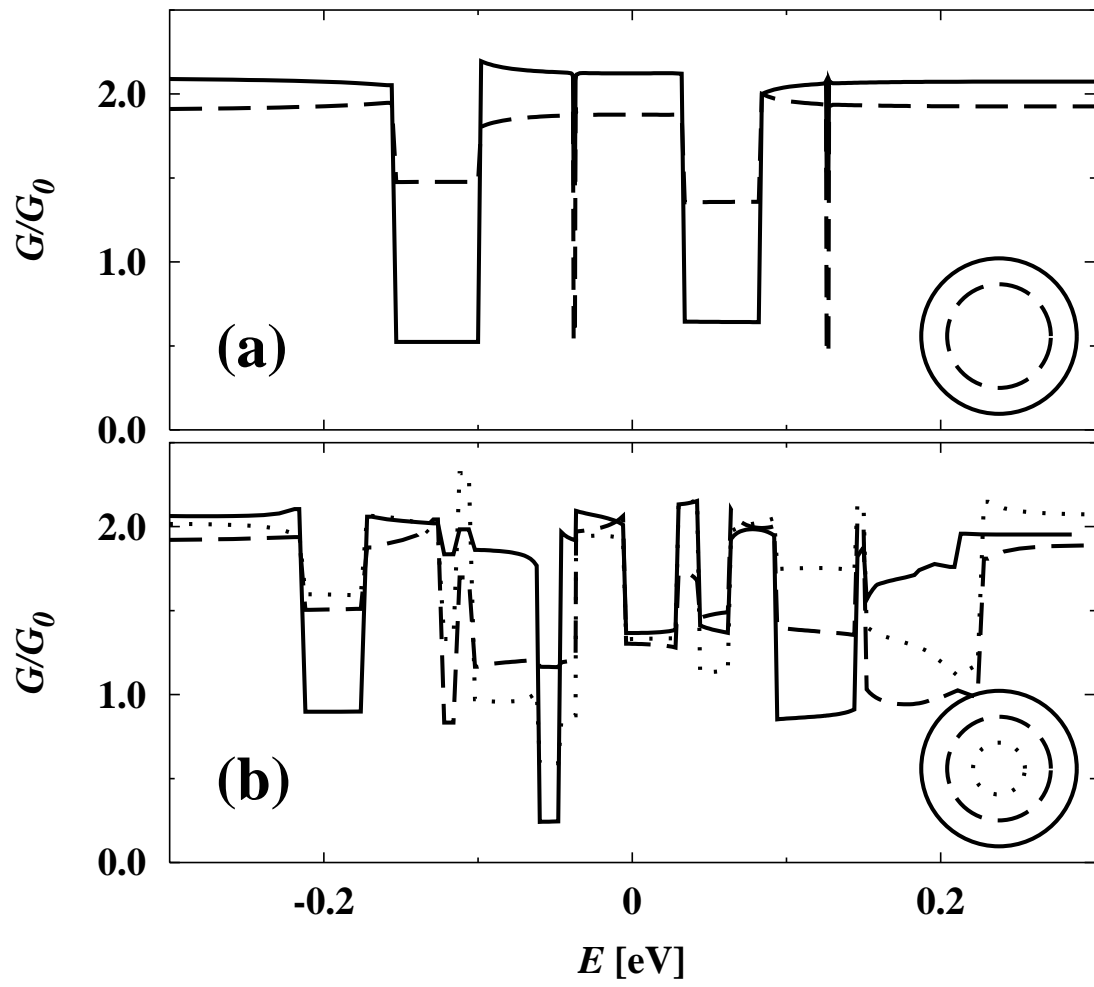


Figure 3

(Stefano Sanvito, Young-Kyun Kwon, David Tománek, and Colin J. Lambert,
“Fractional quantum conductance in carbon nanotubes”)

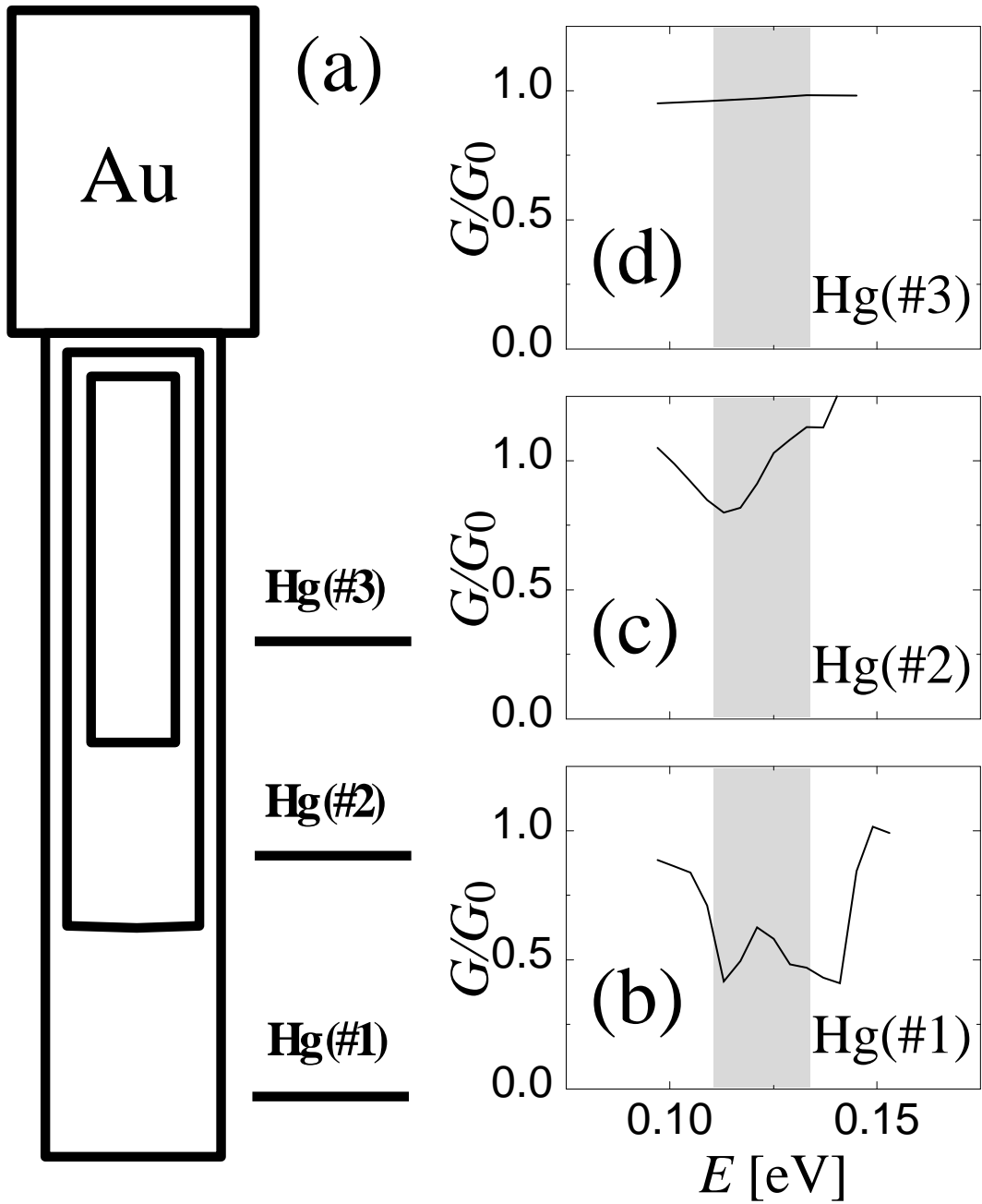


Figure 4

(Stefano Sanvito, Young-Kyun Kwon, David Tománek, and Colin J. Lambert,
"Fractional quantum conductance in carbon nanotubes")

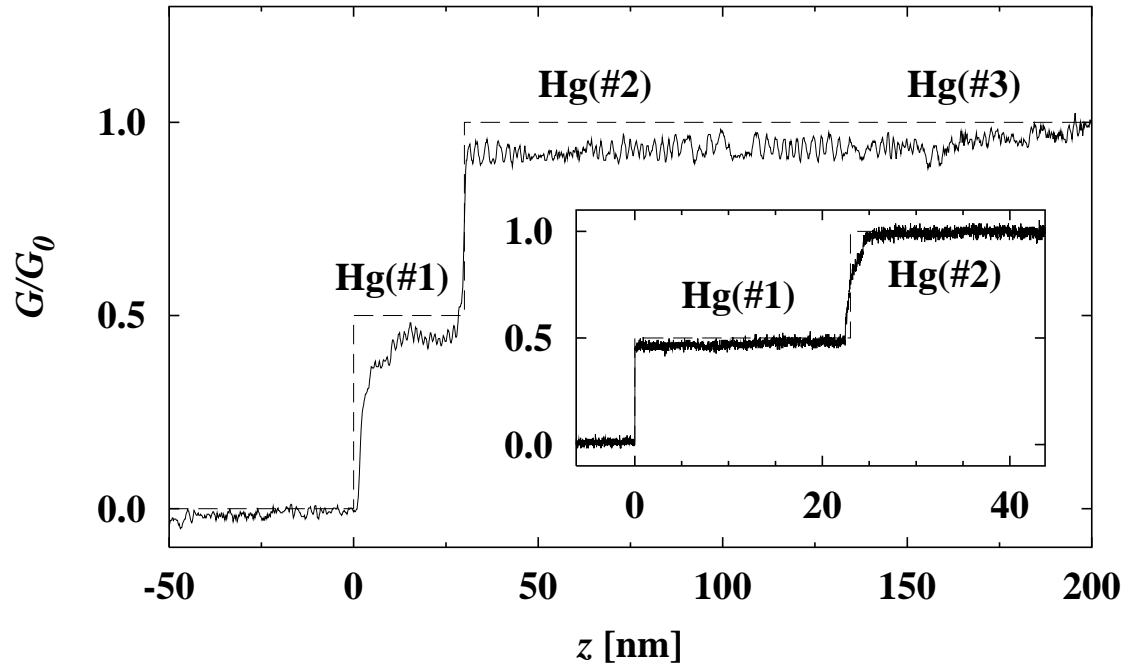


Figure 5

(Stefano Sanvito, Young-Kyun Kwon, David Tománek, and Colin J. Lambert,

“Fractional quantum conductance in carbon nanotubes”)